Struct Multidisc Optim (2012) 45:907–916
DOI 10.1007/s00158-011-0743-7

INDUSTRIAL APPLICATION

Enhanced chain dynamics in loop-sorting-systems by means of layout optimization and a kinematic model of the polygon action

Søren Emil Sørensen · Michael R. Hansen · Morten K. Ebbesen · Ole Ø. Mouritsen

Received: 11 May 2011 / Revised: 29 October 2011 / Accepted: 10 November 2011 / Published online: 8 January 2012

Abstract Poor dynamics owing to polygon action is a known concern in mechanical applications of closed articulated chains. In this paper a kinematic model of the polygon action in large chains of loop-sorting-systems is proposed. Through optimization techniques the chain dynamics is improved by minimizing the polygon action using a parametric model of the track layout as design variables. Three formulations of the kinematic polygon action are tested on an average sized planer tracks layout to find a superior model. Verification of the proposed optimization method is performed using a state-of-the-art multi-body simulation model of the chain dynamics.

Keywords Loop-sorting-systems · Polygon action · Optimization · Multi-body dynamics

1 Introduction

Loop-sorting-systems (LSS) are used for sorting of medium sized items in the business segments of warehouses, post companies and airports. The main component in LSS is the loop-sorter which performs the sorting. The loop-sorter consists of a customized track in which a closed chain of carts drives with a steady speed.

S. E. Sørensen (✉) · O. Ø. Mouritsen
Department of Mechanical and Manufacturing Engineering, Aalborg University, Pontoppidanstraede 105, 9220 Aalborg, Denmark
e-mail: ses@m-tech.aau.dk

M. R. Hansen · M. K. Ebbesen
Department of Engineering, University of Agder, Grooseveien 36, 4876 Grimstad, Norway

M. R. Hansen
e-mail: Michael.R.Hansens@uia.no

The development of customized LSS is a complicated task which requires numerous design iterations to complete. The demands and requirements made by the customer constantly challenge the design engineers. Design of LSS has traditionally been handled through a trial-and-error process which encompasses several design iterations before reaching a final solution. Despite the experienced and dedicated design engineers inappropriateness may still occur in the final design.

A well-known inappropriateness in LSS is poor dynamics in the chain of carts giving rise to increased wear and low durability. The poor dynamics emerges from effects like the polygon action which is an enforced velocity variation in the chain of carts introduced by the discrete links as it changes direction in a curve, see Mahalingam (1958).

The complicated dynamics in the chain of LSS makes it impossible for the design engineer to predict the chain performance by the use of standard means. New methods to predict and improve the chain dynamics are therefore a necessity. In this paper a method to predict and improve the chain dynamics in LSS is proposed. The proposed method optimizes the track layout using a model of the chain dynamics as evaluation criteria. Models of chain dynamics is studied in a wide range of mechanical applications like tracked vehicles and drive trains. A dynamic model of an earthmoving tracked vehicle is presented in Choi et al. (1998). The spatial model uses a formulation of the track treating each link as kinematically decoupled rigid bodies. Each link is connected through revolute joints by which a secondary joint is connected by a force element formulation to avoid a closed kinematic chain. The body interaction between the subsystem of the chassis, the rollers, the sprockets and the idlers and the subsystems of the two tracks is modeled using a penalty formulation, see Lee et al. (1998).

A chain drive model is presented in Pedersen (2005) and Pedersen et al. (2004). Assuming each link of the chain to be lumped masses the chain is modeled using a force element approach. Likewise, the chain interaction with sprockets and guiding bars are modeled using force elements. The chain drive model is tested on a marine diesel engine with convincing results.

A rigid multi-body model of chain dynamics in LSS is presented in Ebbesen (2008). The developed model use theory of unconstrained forward dynamics using a penalty formulation to model contact between each link in the chain and with the track. The model presented in Ebbesen (2008) is further developed in Sørensen et al. (2011a, b) by introducing improved contact formulations. Extensively verification of the model is performed on several test layouts using a special developed sensor cart to measure the chain dynamics in true LSS. Despite the accuracy and robustness of the chain simulations in Sørensen et al. (2011a, b) the dynamic model proves inadequate as evaluation criteria because of insufficient computation time and numeric noise making the design space discontinuous.

In 2006 Ebbesen et al. propose a kinematic model of the polygon action in the chain of carts as a substitute for the dynamic chain model. The kinematic model estimates the polygon action by using an open chain formulation. An estimate of the polygon action is obtained by finding the position of each cart along the track centre line using the relative velocity variation of the last cart in the chain as objective function. By changing the shape of the track layout Ebbesen et al. utilizes the proposed kinematic model as objective function trying to improve the dynamic performance of the chain. Optimization is conducted using the length of the straight tracks and the radii of the curves as design variables. The proposed parametric model of the track layout proves efficient for simple layouts with layout dependent equality constraints to maintain a closed track.

The complex dynamics imposed by the polygon action in LSS should, preferably, be modeled using numerical models, i.e., the criteria related to dynamic performance should be derived from the output of a dynamic model. The problem is that the dynamic chain model in Sørensen et al. (2011a, b) would yield optimization routines that are too lengthy to be used in a practical iterative design phase. Therefore, a kinematic model based on the one presented in Ebbesen et al. (2006) is adopted and the dynamic chain model of Sørensen et al. (2011a, b) is only introduced for verifying purposes. The kinematic model is augmented with new formulations of the polygon action that take local effects between curves into account. The different kinematic formulations are all tested in the proposed optimization method and applied to a practical design example.

2 The topology of LSS

LSS are used for sorting of medium sized items like post packages and luggage by which the main business segments are warehouses, post companies and airports. The main advantages of LSS are their ability to handle a large number of items with a large variation in the shape and size. The main components of LSS are inductions, loop-sorters and chutes. The loop-sorter takes care of the actual sorting and consists of a closed track in which a closed chain of carts drives with at steady speed, see Fig. 1.

The track is shaped using standard track segments like: straight tracks, horizontal curves, vertical curves and spiral curves. A typical track layout is illustrated in Fig. 2. A track

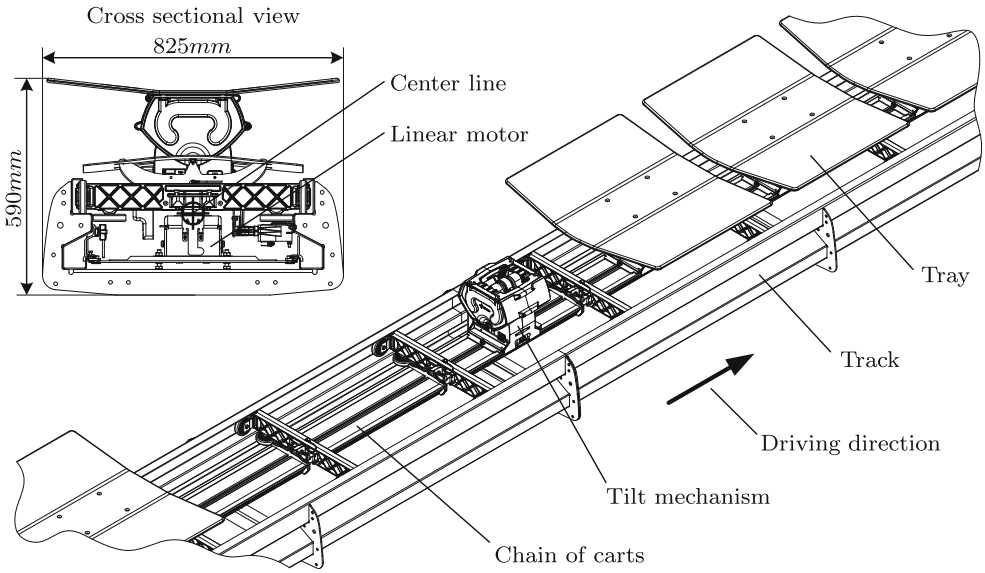

Fig. 1 Cross sectional and isometric view of the loop-sorter

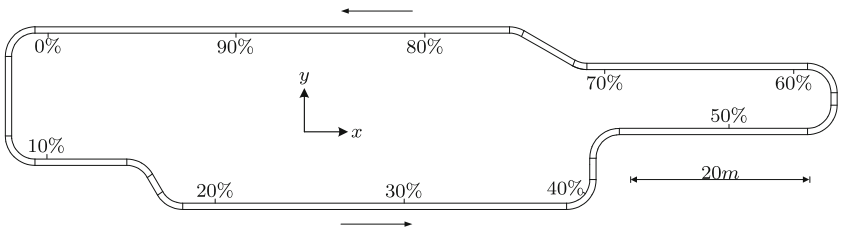

Fig. 2 Typical shape of a LSS track layout. The *parallel polylines* illustrates the track layout while *arrows* alongside indicates the driving direction

layout is shaped according to the sorting task and may range in length from 100 up to 3,000 m.

A link in the chain consists of a cart and a carrier. The cart interfaces to the adjacent links thought a spherical plain bearing and interfaces to the tracks through four wheel mounted on the end profile of the cart, see Fig. 3. The carrier is mounted on the cart and consists of a tilting device and a tray. The cart and the carrier range in length between 500 and 1,250 mm which is defined by the item mix.

Inductions are located along the loop-sorter and this is where the items are guided onto the tray of the carrier. The inducted items are transported by the chain of carts until they reach a defined destination along the track. At the destination the tilting device is activated and the item is discharged into a chute. Several chutes may be located along the track depending on the number of required destinations.

The chain of carts is propelled by stationary linear motors that apply a magnetic force to an iron core located at the bottom of each cart. The linear motors are mounted in the bottom of the track and are evenly distributed along the straight track sections. A closed loop PID control is used to maintain a steady speed of the chain by which the reference speed may be between 1.0 and 3.0 m/s. The input to the PID controller is the speed error and the output is the magnetic force of the linear motors.

3 Model of chain dynamics

The dynamic chain model applies the theory of unconstrained forward dynamics with a force element formulation to model the body interaction. Each cart in the chain is a rigid body by which deformation restricted to small regions around a predefined number of candidate points of contact. Seven contact points on each cart is used to model the chain dynamics, see Fig. 4. The contact points encompasses the left and right steering wheel, the left and right

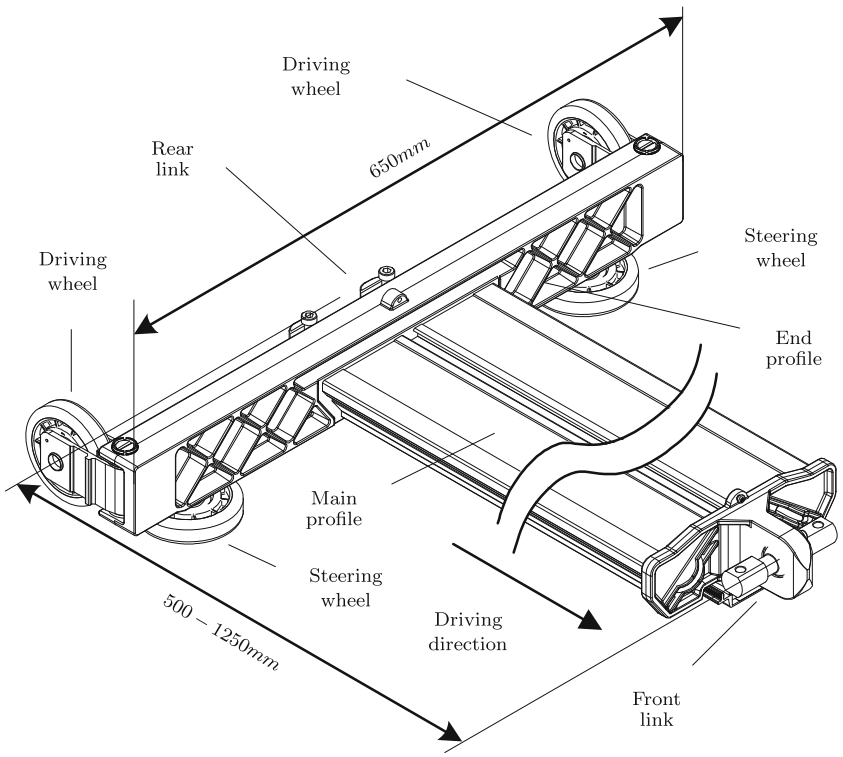

Fig. 3 The design of a cart in the loop-sorter

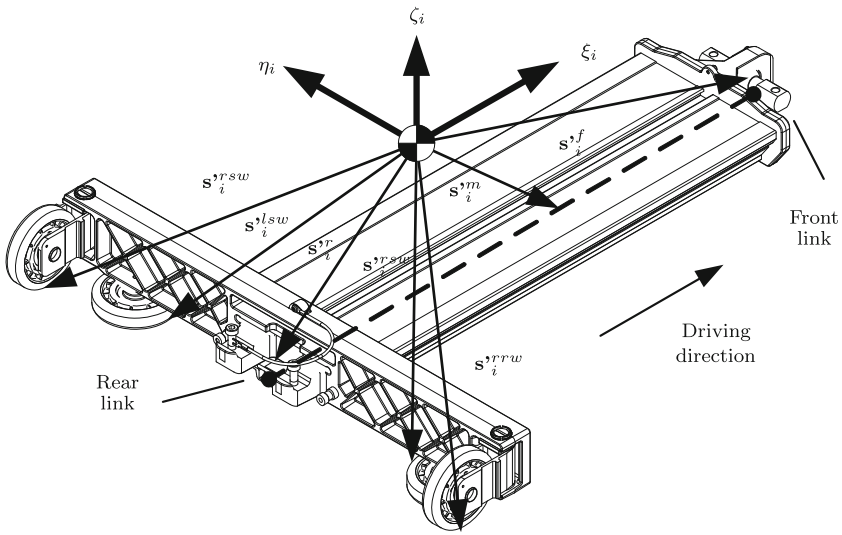

Fig. 4 Local vectors from the carts centre of gravity to the seven points of contacts

running wheel, the front and rear joint and the bottom of the cart. The contact point of the bottom of the cart is shifting depending on the carts location in accordance with the motor.

In each time step a search algorithm identifies all contact within the chain of carts. To search the wheel contact, a kinematic formulation of the track layout is utilized assuming the track to be rigid and all track sections to by perfectly aligned and tangent to each other. The wheel and joint contacts are modeled using the continuous Hunt-Crossly formulation in which the contact force are computed by the indentation and the indentation velocity between the intersecting bodies, see Hunt and Crossley (1975). The motor force is applied as a point force onto the bottom of all carts located above a linear motor.

The kinematic decoupled formulation yields six independent differential equation of motions for each cart which is solved numerically using an explicit fifth order solver provided by Press et al. (1996).

Extensive work is conducted on parameter identification and verification of the dynamic chain model, see Sørensen et al. (2011b). Verification is performed on seven physical systems utilizing a special developed sensor cart to measure seven contact forces in the chain. The experimental work is used for identification of damping parameters by minimizing the residual between measured and simulated forces. Convincing results from the performed verifications confirms the accuracy and robustness of the chain simulation model as evaluation tool.

4 Kinematic model of the polygon action

The polygon action is a kinematic phenomenon which emerges in curves and depends on: the length of the chain links, the curve radius and the curve sweep angle. It is a sinusoidal continuous velocity variation which oscillates with the same frequency as the passing carts. All curves in a track layout produces polygon action of different magnitude with that same frequency but with different phases.

The polygon action is defined as the velocity variations observed in the chain if it is kinematically opened and is repetitive within one cart travel along a straight segment of the track. It is obtained numerically by moving the chain of carts forward in finite steps, Δl_{step}, along a reference straight segment and comparing the deviation in cart motion along the remaining straight sections of the track.

The kinematic model of the polygon action is divided into two parts. The initial part locates the position of each carts front joint along the centre line of the track layout. The second part extracts the polygon action for a single cart on each straight section. The following assumptions are made in the kinematic model:

- The cart joints are located on the centre line of the track.
- All carts have the same length.
- The track is modeled by its centre line in which all track elements are aligned and tangent to each other.

These assumptions of course simplify the kinematics compared with the true kinematics in the chain. Assumption one will impose the most significant simplification because the joints located in a curve in a true system are offset a few millimeter from the centerline. To deal with this assumption a different kinematic formulation that is less computational efficient is required. Assumption two and three are the means of dealing with production tolerances within the true system which has proven less significant.

The finite position of each joint along the track centre line is determined using a numeric solver. A dimensionless coordinate $0 \leq s \leq n_{\text{Seg}}$ defines all points along the

centre line of the entire track. The maximum value of s is the number of segments, n_{Seg}, and s is cyclic, i.e.:

$$\begin{aligned} &if\ s > n_{\text{Seg}} \quad \text{then} \quad s = s - n_{\text{Seg}} \\ &if\ s < 0 \qquad \text{then} \quad s = s + n_{\text{Seg}} \end{aligned} \tag{1}$$

The segment number, i, that corresponds to any s value is simply:

$$i = RNDZ(s) + 1 \tag{2}$$

where $RNDZ$ rounds s towards zero.

Hence, if the i'th track segment corresponding to an s-value is a straight track section then the coordinate on the track is defined by

$$\mathbf{r}(s) = \mathbf{r}_i^0 + (s + 1 - i) \cdot \mathbf{u}_i \cdot l_i \tag{3}$$

where $\mathbf{r}_i^0$ is the starting point of the track section, $\mathbf{u}_i$ is the unit direction vector and l_i is the length of the track segment, see Fig. 5.

Similar formulations like (3) of horizontal curves, vertical curves and spiral curves are available, and may be found in more detail in Ebbesen (2008).

Starting from a predefined point on the track each cart in the chain is positioned along the track centre line in sequential order. The starting point, $\mathbf{r}_j$, of the j'th cart can be found iteratively from the starting point of the $(j-1)$'th cart as:

$$l(s_j) = l_C \tag{4}$$

in which l_C is the cart length and $l(s_j)$ is derived by

$$l(s_j) = \|\mathbf{r}_j(s_j) - \mathbf{r}_{j-1}\| \tag{5}$$

Equation 3 is solved for s_j using the Newton-Raphson iteration method, see Fig. 5.

This way the coordinates of all carts are computed for a given position of the entire chain. For each cart the joint coordinate, $\mathbf{r}_j$, the s-parameter s_j and the segment number i are known. To derive the polygon action the chain is moved forward in finite step $\Delta l_{\text{step}} = l_C / n_{\text{step}}$, by which all joint positions are calculated. The finite steps, k are computed n_{step} times. Test shows that $n_{\text{step}} = 50$ is sufficient to get an accurate representation of the polygon action for a 1,250 mm cart. As the polygon actions are repetitive within a straight section they can be derived from the variation in coordinates of a select number of carts, i.e, one for each straight section. Each of the straight sections may, in turn, be chosen as reference section and the polygon action captured on the remaining straight sections. If n_{SS} is the number of straight sections, such that $n_{SS} < n_{Sec}$, then there is potentially n_{SS} times n_{SS} different polygon actions. The coordinates of the select number of carts is denoted as: $\mathbf{r}_{i,j}^{(k)}$ where i is the straight section used as reference, j is the straight section containing the cart and k is the finite step. This is illustrated in Fig. 6 where straight Section 1 is used as reference and the polygon action for some k'th step is shown in straight Sections 2 and 3.

The polygon action is action at the current step, $p_{i,j}^{(k)}$, see Fig. 6, is computed as:

$$p_{i,j}^{(k)} = \|\mathbf{r}_{i,j}^{(k)} - \mathbf{r}_{i,j}^{(1)}\| - (k-1) \cdot \Delta l_{\text{step}} \tag{6}$$

in which $p_{i,j}^{(k)}$ is the variation between the travel of the reference cart and the cart of the j'th segment at the k'th step. The polygon action of the j'th straight segment relative to the i'th straight segment is simply defined as the maximum absolute value of $p_{i,j}^{(k)}$, as

$$\Delta p_{i,j} = \max|p_{i,j}^{(k)}|, k = 1 \ldots n_{\text{step}} \tag{7}$$

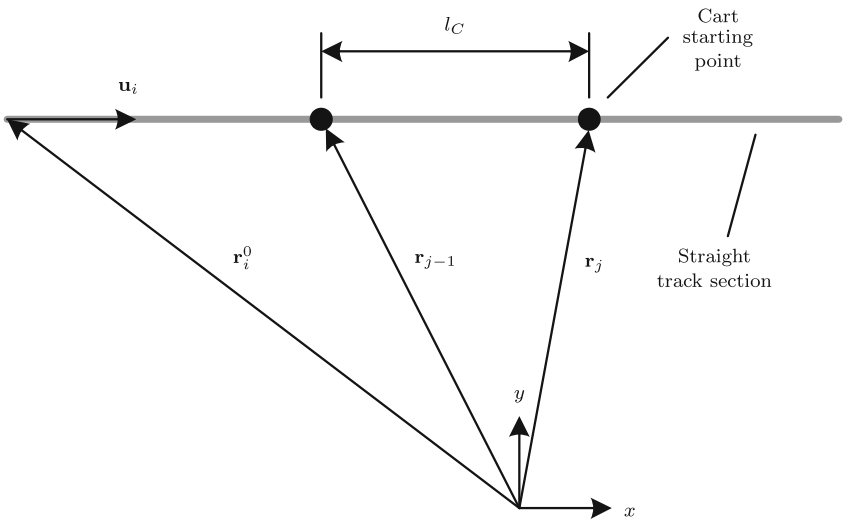

Fig. 5 A straight track section is defined by the variables $\mathbf{r}_i^0$, $\mathbf{u}_i$ and l_i. The cart starting point, $\mathbf{r}_j$ on the track is numerically obtained by the track function definitions and the starting point of the previous cart, $\mathbf{r}_{j-1}$ using a Newton Raphson solver

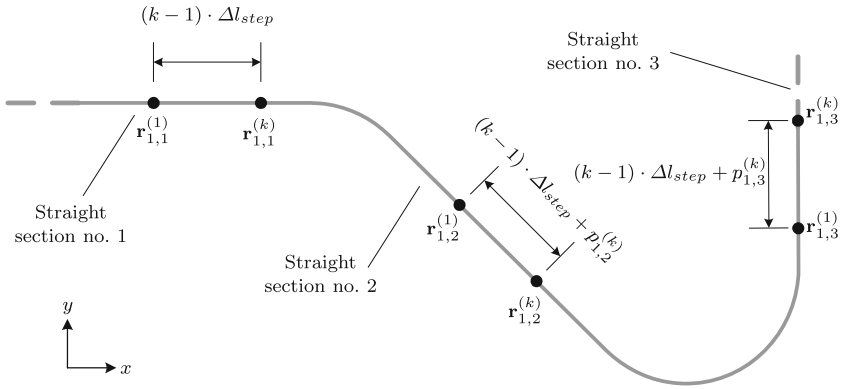

Fig. 6 The polygon action illustrated for the first three straight sections with the first section used as reference

This yields a square matrix of polygon actions with dimension equal to n_{SS} and with zero elements in the diagonal.

5 Formulation of the optimization problem

The design of LLS is, in general, complex and multidisciplinary. There are a number of side constraints associated with the wide variety of three-dimensional obstacles that may not collide with the track, the inductions and the chutes. Therefore, the design of an LLS is an iterative process in which it is often required to optimize the dynamic performance for a given track layout that is in accordance with the geometric constraints of the surroundings. In that case the improvement of the dynamic performance may be formulated as a minimization problem:

$$\begin{aligned} &\underset{\mathbf{x}}{\text{minimize}} \quad f(\mathbf{x}), \qquad \mathbf{x} \in \mathbb{R}^m \\ &\text{subject to} \quad \mathbf{g}_i(\mathbf{x}) \leq \mathbf{0}, \; i = 1, \ldots, m_2 \end{aligned} \tag{8}$$

in which $f(\mathbf{x})$ is the objective function evaluating the dynamic performance in the chain of carts and $\mathbf{x}$ are the design variables of the track layout. The optimization problem is subject to a set of inequality functions $\mathbf{g}(\mathbf{x})$ which constrain the design variables to maintain within plausible track layouts. The inequality constraints are embedded in the objective function using a penalty formulation.

As the kinematic formulation of the polygon action is an approximation of the true chain dynamics three formulation of the objective function are tested to find the most suitable model. The three formulations test the effect of the polygon actions interference between curves by evaluating various combinations of entrances in $\Delta p_{i,j}$. Objective function 1, $f_1(\mathbf{x})$ is formulated as the root mean square of all entrances of $\Delta p_{i,j}$, by

$$f_1(\mathbf{x}) = \sqrt{\frac{\sum_{i=1}^{n_{SS}} \sum_{j=1}^{n_{SS}} \Delta p_{i,j}^2}{n_{SS} \cdot n_{SS}}} \tag{9}$$

in which n_{SS} is the number of straight track sections. The interference between the first three curves after the starting point is evaluated in objective function 2, $f_2(\mathbf{x})$ by

$$f_2(\mathbf{x}) = \sqrt{\frac{\sum_{i=1}^{n_{SS}} \sum_{j=1}^{3} \Delta p_{i,j}^2}{3 \cdot n_{SS}}} \tag{10}$$

A modified version of the formulation presented in Ebbesen (2008) is utilized in objective formulation 3, by which the polygon action of the last cart in the chain is defined as

$$f_3(\mathbf{x}) = \sqrt{\frac{\sum_{i=1}^{n_{SS}} \Delta p_{i,n_{SS}}^2}{n_{SS}}} \tag{11}$$

The optimization problem is solved using the non-gradient Complex algorithm, see Box (1965) and Manetsch (1990). The Complex algorithm applies a population of design candidates which evolves towards the optimum by constantly replacing the worst design candidate. The new design candidate is found by mirroring the worst candidate over the center of the remaining candidates in the design population. An optimum is reached when the difference in the objectives of the design populations is $\delta < 10^{-4}$. A design population of $m + 2$ is used where m is the number of design variables.

Explicit constraints are not used in the optimization problem as the objective formulations hold multiple optimum solutions close to the initial track layout. However, to reach a solution close to the original track layout the initial random generated population of design candidates is constrained to be within ± 1.0 m of the original design variables. The design candidates are allowed to move outside this region as the population evolves towards an optimum.

6 Test layout

A planar layout is use as initial design candidate for the proposed layout optimization method, see Fig. 2. The two

closed parallel lines outline the track sides while perpendicular lines within illustrate the start and termination of each track section. Arrows along the track indicate the driving direction of the chain and figures along the track indicate the distance from the trigger point. This trigger point is utilized by the dynamic chain model to start and terminate the simulation. The track layout is 214.0 m long and consists of ten straight sections, seven horizontal curves turning left and three horizontal curves turning right which all are 3 m in radius. The chain consists of 171 carts which each weighs 40 kg and has an average length of 1,250 mm. The chain of carts is propelled by 12 linear motors that are controlled based on a target chain speed of 1.9 m/s.

7 Parametrization of the track layout

The parametric formulation proposed in Sørensen et al. (2011c) is utilized to get a set of independent design variables of the track layout. In order to get at set of continuous design variables the discrete sweep angles of the horizontal curves are relaxed to encompass any angle. The track layout is parameterized by using the Euclidian coordinates (x_q, y_q) of vertices $P_1, P_2, ..., P_{n_q}$ located at the intersection points of the neighboring straight track sections, see Fig. 7. The radii of the curves, R_q are not as in Sørensen et al. (2011c) used as design variables as only three discrete options are commercially available. Ten vertices are used to parameterize the test layout which gives a total of $m = 20$ design variables.

Two types of geometrical inequality constraints are defined to ensure plausible shapes of the track layout. The distance between the neighboring vertices are constrained to avoid curves from overlapping by

$$0 \geq h_q + h_{q+1} - |\mathbf{d}_q| \tag{12}$$

in which $\mathbf{d}_q$ is the vector

$$\mathbf{d}_q = \begin{bmatrix} x_{q+1} - x_q \\ y_{q+1} - y_q \end{bmatrix} \tag{13}$$

and h_q is the arc line defined by

$$h_q = R_q \cdot \tan\left(\frac{\alpha_q}{2}\right) \tag{14}$$

The angle α_q is obtained by

$$\cos(\pi - \alpha_q) = (-\mathbf{u}_q) \cdot \mathbf{u}_{q+1} \tag{15}$$

where $\mathbf{u}_q$ is the unit vector of $\mathbf{d}_q$. To prevent acute angles between straight track sections the angle α_q is constrained by

$$0 \geq \alpha_q - \frac{3\pi}{4} \tag{16}$$

The relaxed parametric formulation entails solutions which do not fulfill a multiple of 2.5° of the curve sweep angles. Consequently, the penalty method adopted in Sørensen et al. (2011c) should be applied to reach a track layout which matched the discrete sweep angles of the standard track elements.

8 Results

The stochastic Complex algorithm and the non-convex design space entails that the optimization problem may converge at different solutions. Accordingly, the optimization problem is executed ten times for every formulation of the objective function.

Table 1 shows the results for the three formulation of the objective function. The first column shows the average, maximum and minimum percentage reduction from

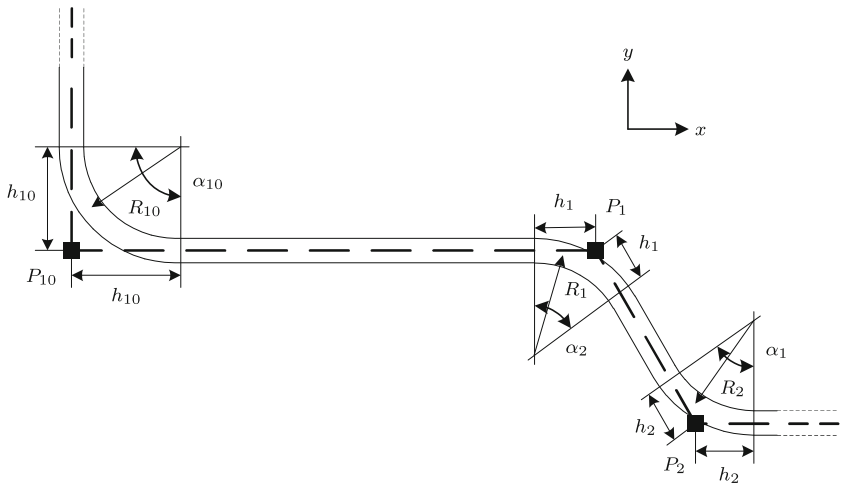

Fig. 7 *Lower left part* of the test layout. The intersection points of the neighboring straight track section are used as design variables

Table 1 The percentages reduction from the initial value of the three objective functions of ten repetitions

	Kinematic model*			Number of iterations			FFT**			Rainflow ***		
	Avg. (%)	Max. (%)	Min. (%)	Avg.	Max.	Min.	Avg. (%)	Max. (%)	Min. (%)	Avg. (%)	Max. (%)	Min. (%)
Objective 1	79	91	74	7,124	11,876	3,515	76	88	56	44	58	11
Objective 2	87	92	69	6,029	10,440	3,767	69	83	48	41	58	19
Objective 3	98	99	95	6,632	10,676	3,764	65	82	43	38	55	13

*Improvements in the kinematic polygon action
**Improvements in the magnitude of the main frequency of longitudinal forces in the cart joint
***Improvements in the equivalent force of the joint in longitudinal direction

the initial value of the three objective functions. The second column show the number of iteration conduction before reaching the optimum solution. It is shown by the results that the polygon action improves quite significantly for all three formulations in which every solution are reduced more than 69%. Through comparisons of the three objective functions the least significant reductions in the polygon action are obtained by function 1 while function 3 reached the greatest reduction. All three formulations utilize approximately the same amount of iteration to reach an optimum solution.

To verify the applicability of the three objective functions the initial and optimum solutions are compared using the dynamic chain simulation model. Two figures from the dynamic simulations are compared:

- The magnitude of the main frequency arising from the polygon action of the longitudinal joint forces, see Table 1 column 3.
- The equivalent force in the joint in longitudinal direction using accumulated fatigue (rainflow counting) with a cut-off at $80N$, see Table 1 column 4.

Both the magnitude of the main frequencies and the equivalent force is reduced quite significantly for all three objective functions. The greatest improvements are obtained with objective function 1 while the least significant improvements are obtained with objective function 3. The proposed kinematic model improves the chain dynamics for all three objective functions. Thus, reducing the geometric polygon action by changing the shape of track layout is a very useful approach. The reduced polygon action and the actual improvement indicated by the dynamic model show that a direct relationship between the kinematic model and the dynamic model is unambiguous. As a result it might be necessary to compare results of the dynamic chain model when using the kinematic formulation as evaluation criterion. Especially in complex track layouts with numerous curves involved.

The longitudinal joint force for the initial (gray line) and the optimum result (black line) using objective function 3 is shown in Fig. 8. It is significant how fluctuation in the joint force is reduced for the optimum track layout in which the force amplitude is reduced to under the half.

The significant reduction in the force fluctuations is also shown from the Fast Fourier Transform (FFT) of the longitudinal joint forces, see Fig. 9. The gray line illustrates the frequency spectra for the initial track layout while the black line illustrates the frequency spectra of the best solution obtained with objective function 2. The three peaks originate from the polygon action and have the frequency corresponding to $1/1$, $1/2$ and $1/3$ of the cart length. A significant reduction in the first two peaks is achieved by the optimized track layout.

The reduced chain dynamics is also observed in the contact force on the steering wheel. Figure 10 shows the steering wheel force perpendicular to the driving direction by which a negative force is contact on the left steering

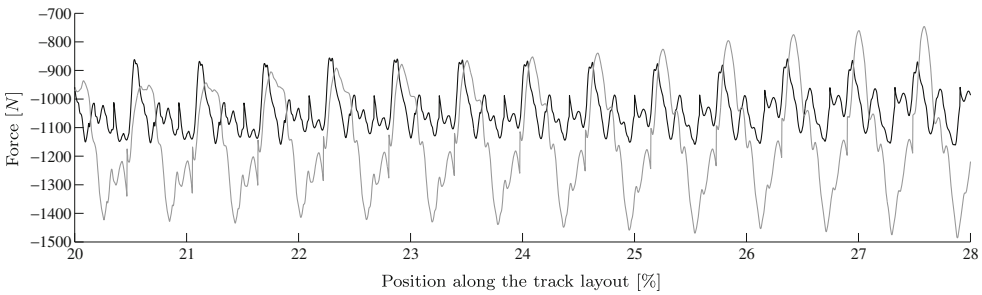

Fig. 8 Initial (*gray*) and optimum (*black*) longitudinal forces in the cart joints. The optimum force is the best solution obtained with objective function 3

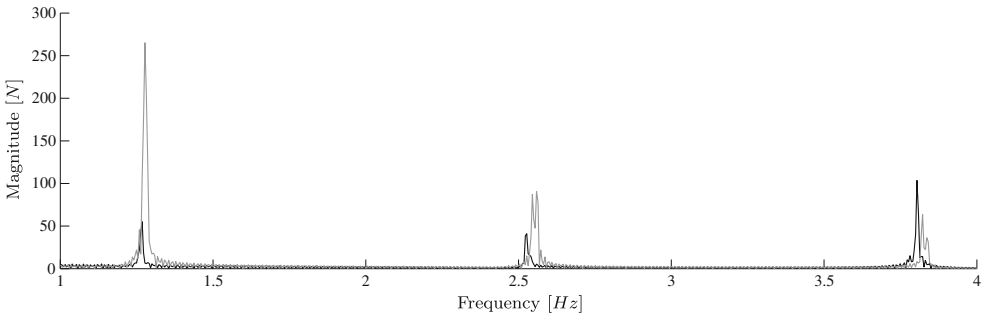

Fig. 9 FFT analysis of initial (*gray*) and optimum (*black*) longitudinal Forces in the cart joints. The optimum force is the best solution obtained with objective function 2

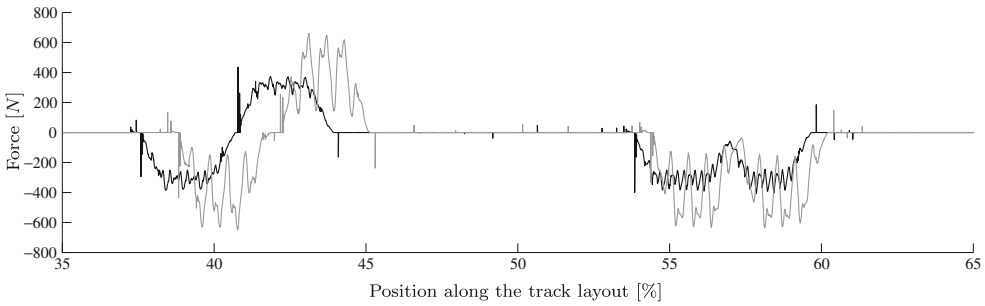

Fig. 10 Initial (*gray*) and optimum (*black*) force on left (*negative*) and right (*positive*) steering wheel. The optimum force is the best solution obtained with objective function 1

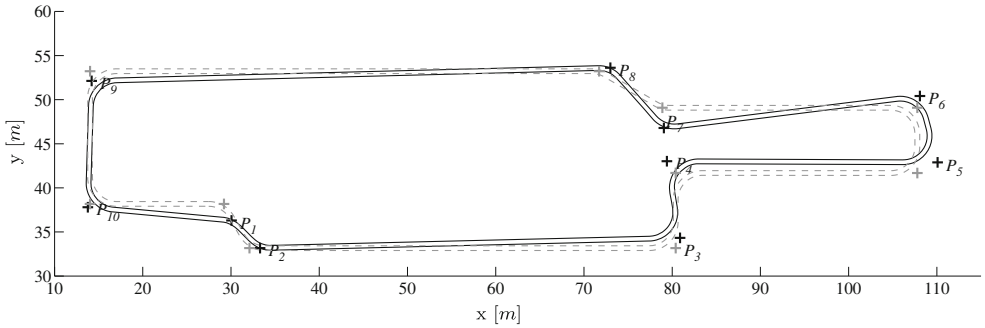

Fig. 11 Track layout (*black lines*) of best optimum solution with objective formulation 1. The *gray dotted lines* show the initial track layout

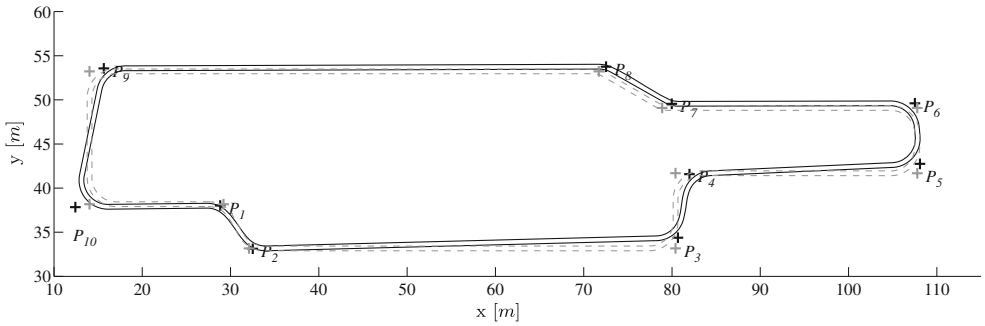

Fig. 12 Track layout (*black lines*) of best optimum solution with objective formulation 2. The *gray dotted lines* show the initial track layout

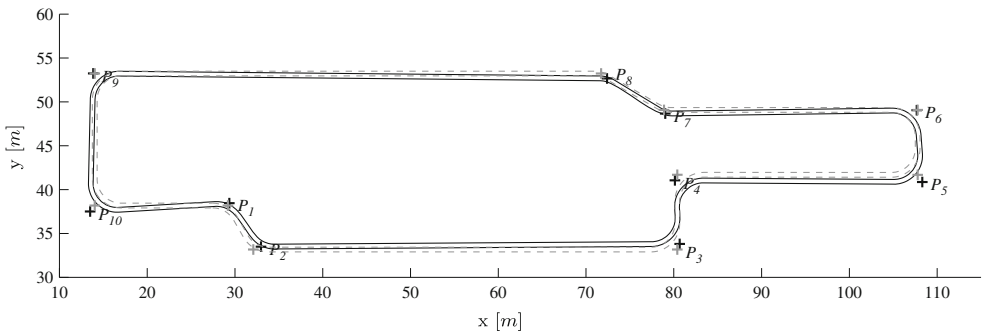

Fig. 13 Track layout (*black lines*) of best optimum solution with objective formulation 3. The *gray dotted lines* show the initial track layout

wheel and a positive force is contact on the right steering wheel. The gray line show the contact forces for the initial track layout while the black line shows the best result obtained with objective function 1. The polygon action in the initial track layout introduces grate force variations in the steering wheel contact. The large force variations are reduced significantly in the optimized track layout.

Figures 11, 12 and 13 shows the best solutions of the track layout for the three objective functions. The black lines show the optimized track layout while the dotted gray lines illustrate the initial track layout.

All performed optimizations reach a solution close to the original track layout. However, all three solutions differ in shape which shows the large number of local minima's introduced by the kinematic formulation of the polygon action.

9 Conclusion

A method for optimization of chain dynamics in LSS has been proposed. The proposed method minimizes poor dynamic introduced in the chain of carts due to the polygon action. A kinematic model of the polygon action in the chain of carts has been developed as evaluation criteria in which three formulations are tested to find the superior model.

The poor dynamics are minimized by changing the shape of the track layout reducing the interference of the polygon action between curves. A parametric formulation using vertices of the intersection point between the neighboring straight track sections has been utilized.

Results show significant reduction in the polygon action for all three kinematic models with the least improvements as high as 69%. These improvements are confirmed by the dynamic chain simulations where significant reductions in the force fluctuation are observed. Yet, improvements obtained by the kinematic models do not have a direct relationship with the improvements shown by the dynamic simulation.

Three objective function has been tested to find the superior representation of the chain performance. The kinematic model used in objective function 1 generates in general superior results by which this formulation is recommended. All optimum solutions only encompasses small changes to the initial track layout by which the proposed optimization method are applicable in a late stage of the design process of LSS.

Acknowledgments We would like to thank the Danish Agency for Science Technology and Innovation (www.fi.dk) for financing the industrial Ph.D. project "Automatic Design of Sorting Systems". We would also like to thank Crisplant A/S (www.Crisplant.com) for being most kind in providing information and materials for the presented optimization method.

References

Box MJ (1965) A new method of Constrained optimization and comparison with other methods. Comput J 8:42–52

Choi JH, Lee HC, Shabana AA (1998) Spatial dynamics of multibody tracked vehicles part I: spatial equations of motion. Veh Syst Dyn 29(1):27–49

Ebbesen MK (2008) Optimal design of flexible multibody systems. PhD thesis, Department of Mechanical Engineering, Aalborg University, Denmark

Ebbesen MK, Hansen MR, Pedersen NL (2006) Design optimization of conveyor systems, III European conference on computational mechanics solids. Structures and coupled problems in engineering. Lisbon, Portugal, pp 5–8

Hunt KH, Crossley FRE (1975) Coefficient of restitution interpreted as damping in vibroimpact. ASME J Appl Mech 42:440–445

Lee HC, Choi JH, Shabana AA (1998) Spatial dynamics of multibody tracked vehicles part II: spatial equations of motion. Veh Syst Dyn 29(2):113–137

Manetsch TJ (1990) Toward efficient global optimization in large dynamic systems—the adaptive complex method. IEEE Trans Syst Man Cybern 20(1):257–261

Mahalingam S (1958) Polygonal actions in chain drives. J Franklin Inst 265:23–28

Pedersen SL (2005) Model of contact between rollers and sprockets in chain-drive systems. Appl Mech 74:489–508

Pedersen SL, Hansen JM, Ambrósio AC (2004) A roller chain drive model including contact with guide-bars. Multibody Syst Dyn 12:285–301

Press WH, Teukolsky SA, Vetterling WT, Flannery BP (1996) Numerical recipes in fortran 90: the art of parallel scientific computation, 2nd edn. Cambridge University Press

Sørensen SE, Hansen MR, Ebbesen MK, Mouritsen OØ (2011a) Time domain simulation of large scale material handling chains using an unconstrained formulation. J Multi-body Dyn 225:95–110

Sørensen SE, Hansen MR, Ebbesen MK, Mouritsen OØ (2011b) Implicit identification of contact parameters in a continuous chain model. MIC 32(1):1–15

Sørensen SE, Hansen MR, Ebbesen MK, Mouritsen OØ (2011c) Non-linear optimization of track layouts in loop-sorting-systems. Journal of Automation in Construction (Under revision. submitted april 2011)